LLNL-PROC-694045

LAWRENCE LIVERMORE NATIONAL LABORATORY

Uncertainty Analysis of Signal Deconvolution Using A Measured Instrument Response Function

E. P. Hartouni, B. Beeman, J. A. Caggiano, C. Cerjan, M. J. Eckart, G. P. Grim, R. Hatarik, A. S. Moore, D. H. Munro, T. Phillips, B. D. Sayre

June 2, 2016

21st Topical Conference on High-Temperature Plasma Diagnostics
Madison, WI, United States
June 5, 2016 through June 9, 2016

Uncertainty Analysis of Signal Deconvolution Using A Measured Instrument Response Function [a)]

E. P. Hartouni [b)], B. Beeman, J. A. Caggiano, C. Cerjan, M. J. Eckart, G. P. Grim, R. Hatarik, A. S. Moore, D. H. Munro, T. Phillips, D. B. Sayre

Lawrence Livermore National Laboratory, Livermore, California, 94550, U.S.A.

(Presented XXXXX; received XXXXX; accepted XXXXX; published online XXXXX)

A common analysis procedure minimizes the ln-likelihood that a set of experimental observables matches a parameterized model of the observation. The model includes a description of the underlying physical process as well as the instrument response function (IRF). In the case investigated here, the National Ignition Facility (NIF) neutron time-of-flight (nTOF) spectrometers, the IRF is constructed from measurements and models. IRF measurements have a finite precision that can make significant contributions to the uncertainty estimate of the physical model's parameters. We apply a Bayesian analysis to properly account for IRF uncertainties in calculating the ln-likelihood function used to find the optimum physical parameters.

I. INTRODUCTION

A. NIF Measurements

The National Ignition Facility (NIF) provides up to 2 MJ of 3ω (351 nm) laser light to a variety of targets including hohlraums containing spherical capsules, and also directly to spherical capsules[1,2]. The capsules are filled with various mixtures of deuterium, tritium and ^{3}He fuels that upon implosion create thermonuclear fusion. Neutrons, which are products of the fusion reactions provide diagnostics of the performance of the implosion through their kinetic energy spectrum[3,4,5]. Among the quantities inferred from the neutron spectrum are yield, ion temperature and the cold fuel areal density. Future analyses will attempt to infer information about temperature gradients and fuel motion[6]. The ability to provide physically meaningful quantities depends on the analysis of the uncertainties with which these quantities are determined from the spectrum measurements.

B. NIF nTOF spectrometers

The NIF nTOF spectrometers[9-11] are deployed in 5 lines-of-sight (LOS) at different polar- and azimuthal-angles around the Target Chamber Center (TCC). Each LOS is collimated providing a narrow view of the target at TCC, thus eliminating backgrounds from neutron interactions with material within the target chamber. The spectrometers occupy radial distance from 18 to 27 m. For 4 spectrometers, a bibenzyl scintillator which is under-filled by the collimated LOS is viewed with 4 photo-detectors of varying sensitivity. These photo-detectors are located out of the LOS and are shielded from the primary radiations originating at the target. Provisions for inserting a neutral density (ND) filter allows the ability to adjust the photo-detector sensitivities to the specific shot design.

The photo-detector signals are propagated along coax cables of varying length to a digital oscilloscope, one for each photo-detector, where the wave-forms are recorded and stored until readout. The four channels on each oscilloscope are set to record each detector signals at varying sensitivity, and each channel has a fiducial timing mark added to provide temporal alignment. These four channels can be used to expand the dynamic range of the digitizers through a "stitching" algorithm.

II. NTOF ANALYSIS

The signals are analyzed using a "forward fitting" procedure[7]. A relativistic model for the neutron spectrum contains four parameters: amplitude, ion temperature, central time and a scattering coefficient. The LOS attenuation and the modeled detector sensitivity, as functions of neutron kinetic energy, are applied to the neutron spectrum and transformed into time-of-flight to provide a prediction of the neutron flux at the scintillator. This flux is then convolved with the IRF to provide a model of the digitized signals.

The parameters are optimized by a Least-Squares method formed from the difference of the observed signal and the model predictions.

The uncertainty of the parameters is estimated by scaling the Least-Square value by the signal uncertainty as determined by the digitizer noise, assuming it is the dominant noise source. These uncertainty estimates have been determined to be underestimates of the actual statistical variation of the fit model parameters by various tests. However, the uncertainties of the LOS attenuation, scintillator sensitivity and the IRF are not taken into account.

The analysis performed for this contributed paper calculates the ln-likelihood function including these sources of uncertainties.

[a)] Contributed paper published as part of the Proceedings of the 21st Topical Conference on High-Temperature Plasma Diagnostics (HTPD 2016) in Madison, Wisconsin, USA. LLNL-PROC-694045 prepared by LLNL under Contract DE-AC52-07NA27344.
[b)]Author to whom correspondence should be addressed: hartouni1@llnl.gov.

III. BAYESIAN ANALYSIS

The starting point for this analysis identifies the signal time-series as a vector $\boldsymbol{s}$ with N_s components. The statistical variation of each component is assumed to be normally distributed and additive (with mean of zero). Similarly, the IRF is taken to be a vector $\boldsymbol{h}$ of N_h components, also normally distributed. The model of the signal in the time domain is used to form a matrix that transforms the IRF vector into a prediction of the signal vector:

$$\mathbf{s} = \mathbf{M}\mathbf{h} + \mathbf{e}_s \tag{1}$$

where $\boldsymbol{e_s}$ is the noise vector and the N_s x N_h matrix $\boldsymbol{M}$ is the Toeplitz matrix:

$$M = \begin{pmatrix} m_0 & 0 & 0 & \cdots \\ m_1 & m_0 & 0 & \cdots \\ m_2 & m_1 & m_0 & \cdots \\ \vdots & \vdots & \vdots & \ddots \end{pmatrix} \tag{2}$$

is built from the model time-series vector of length N_s. Presuming that the measured IRF represents a single member selected from a statistical population of IRFs based on variations about the "exact" IRF, we write:

$$\mathbf{h} = \hat{\mathbf{h}} + \mathbf{e}_h \tag{3}$$

where $\boldsymbol{e_h}$ is the noise vector, and $\hat{h}$ is the "exact" IRF which we do not know.

Bayes' formula provides the posterior probability distribution function (PDF) for the model given the observed signal **s** and the IRF:

$$p(s)p(\mathbf{m}|\mathbf{s},\mathbf{R}_s,\mathbf{h},\mathbf{R}_h) = p(m)p(\mathbf{s}|\mathbf{m},\mathbf{R}_s,\mathbf{h},\mathbf{R}_h) \tag{4}$$

where $p(m)$ and $p(s)$ are the prior pdfs for m and s and R_s and R_h are the covariance matrices for s and h. The pdf $p(s|m,R_s,h,R_h)$ is unknown. However, the pdf of obtaining a signal from the model with the exact IRF would be:

$$p(\mathbf{s}|\mathbf{m},\mathbf{R}_s,\hat{\mathbf{h}}) \sim \mathcal{N}(\mathbf{M}\hat{\mathbf{h}},\mathbf{R}_s) \tag{5}$$

which is the normally distributed signal prediction and the pdf for a particular exact IRF:

$$p(\hat{\mathbf{h}}|\mathbf{h},\mathbf{R}_h) \sim \mathcal{N}(\mathbf{h},\mathbf{R}_h) \tag{6}$$

which is the mean of the population of measured IRFs. These two expression can be used to provide the unknown pdf in Eq.(4):

$$p(\mathbf{s}|\mathbf{m},\mathbf{R}_s,\mathbf{h},\mathbf{R}_h) = \int \mathbf{d}\hat{\mathbf{h}}\; p(\mathbf{s}|\mathbf{m},\mathbf{R}_s,\hat{\mathbf{h}})p(\hat{\mathbf{h}}|\mathbf{h},\mathbf{R}_h) \tag{7}$$

where the integral is over all possible exact IRFs. If we assume that the integrand is also normally distributed:

$$\begin{aligned}&\int \mathbf{d}\hat{\mathbf{h}}\; p(\mathbf{s}|\mathbf{m},\mathbf{R}_s,\hat{\mathbf{h}})p(\hat{\mathbf{h}}|\mathbf{h},\mathbf{R}_h) = \\ &\int \mathbf{d}\hat{\mathbf{h}} \exp\left[\left(\mathbf{s}-\mathbf{M}\hat{\mathbf{h}}\right)^{\mathrm{T}}\mathbf{R}_s^{-1}\left(\mathbf{s}-\mathbf{M}\hat{\mathbf{h}}\right)+\left(\mathbf{h}-\hat{\mathbf{h}}\right)^{\mathrm{T}}\mathbf{R}_h^{-1}\left(\mathbf{h}-\hat{\mathbf{h}}\right)\right]\end{aligned} \tag{8}$$

one can then rearrange the terms isolating those in exact IRF and perform the integration to obtain the pdf corresponding the likelihood function we are interested in:

$$p(\mathbf{m}|\mathbf{s},\mathbf{R}_s,\mathbf{h},\mathbf{R}_h) \propto \frac{p(\mathbf{m})}{|\mathbf{P}|^{1/2}}\exp\left[\left(\mathbf{s}-\mathbf{M}\mathbf{h}\right)^{\mathrm{T}}\mathbf{K}\left(\mathbf{s}-\mathbf{M}\mathbf{h}\right)\right] \tag{9}$$

where the matrices P and K are a result of the rearrangements:

$$\mathbf{P} = \left(\mathbf{M}^{\mathrm{T}}\mathbf{R}_s^{-1}\mathbf{M} + \mathbf{R}_h^{-1}\right)^{-1} \tag{10}$$

$$\mathbf{K} = \mathbf{R}_s^{-1} - \mathbf{R}_s^{-1}\mathbf{M}\mathbf{P}\mathbf{M}^{\mathrm{T}}\mathbf{R}_s^{-1} \tag{11}$$

this likelihood has the form of a generalized χ^2 where the covariance matrix is **K**, modified by the normalization |**P**| representing the integral over all exact IRFs.

This analysis was presented by P. Pernot in the note "Bayesian analysis of signal deconvolution using measured instrument response functions" http://arXiv:physics/0604154v1.

For our purposes we take the ln-likelihood to be:

$$\ln\left[p(\mathbf{m}|\mathbf{s},\mathbf{R}_s,\mathbf{h},\mathbf{R}_h)\right] \propto \left(\mathbf{s}-\mathbf{M}\mathbf{h}\right)^{\mathrm{T}}\mathbf{K}\left(\mathbf{s}-\mathbf{M}\mathbf{h}\right) \tag{12}$$

and minimize this form with respect to variation of the model parameters. Further, the uncertainties of the parameters of the model are found by varying each parameter separately until the value of the ln-likelihood increase by 1 (allowing for asymmetric uncertainties) in correspondence with the usual procedure with χ^2.

Note that where the signal covariance $\mathbf{R_s}=\sigma_s^2\mathbf{I}$ where σ_s is the signal noise, and $\mathbf{R_h} \to 0$ (the limit of "exact" IRF which is currently used), that the ln-likelihood reverts to the χ^2 used by the current analysis.

Another insight of this analysis is that the selection of a single IRF from the population of possible IRFs can bias the parameters. This bias represents an irreducible systematic uncertainty for the parameters that can be calculated in this model. It is important to recognize that the assumed pdf for the distribution of IRFs around the exact IRF is an ansatz which may not be physically realized in the detector system.

However, this analysis provides a framework to explore how uncertainties in the measurement process, as represented by the procedure by which the IRFs are constructed and the estimated covariance of the "measured" IRFs affects the uncertainties in the model parameters.

IV. APPLICATION TO NIF NTOF

The full analysis of the covariance of the signal and the IRF is underway. To make contact with the current analysis it is sufficient to assume a simple covariance model, $\mathbf{R_s}=\sigma_s^2\mathbf{I}$ where the "noise," σ_s, is set to the standard deviation of the wave-form signal (for the first 100 nanoseconds). The covariance of the IRF is similar, $\mathbf{R_h}=\sigma_h^2\mathbf{I}$ where σ_h is set to same fractional uncertainty as the signal, $\sigma_h = (\sigma_s/s_{max})h_{max}$. The absolute value of σ_h is much smaller than σ_s.

The time region in which the fit is performed is varied from 30ns to 70ns in 10ns steps to investigate the convergence of the final results. The "exact" IRF fit is performed first, and the parameters passed to the Bayesian fit. The signal used in the fit is taken from a single digitizer channel chosen to be the highest sensitivity channel which did not saturate.

The optimization was performed by a multidimensional downhill simplex method using a χ^2 like cost function. This cost function was used to find the parameter values where the cost function minimum was increased by 1, corresponding to the integrated likelihood function value of 63%, the definition of 1-σ parameter uncertainties.

V. RESULTS

The practical limit of the implementation of this analysis to the NIF nTOF analysis is set by the matrix operations. For matrix dimensions greater than 800x800 (80 ns of signal and 80 ns of IRF) more precise matrix operation algorithms will need to be employed. The parameter values for each fitting procedure converge for time regions greater than or equal to 40 ns, so this limit does not affect this study.

TABLE I. Result of fitting using the two techniques for nTOF SPEC-Alcove, detector 2 on the DT "layered" shot N160418-001-999.

Parameter	Value	Upper 1-σ	Lower 1-σ
"Exact"			
Amplitude (A)	0.544	0.003	0.003
t_0 (ns)	449.78	0.023	0.023
T_{ion} (keV)	4.720	0.055	0.055
Scatter coef.	0.613	0.092	0.091
χ^2/ndof	0.334		
"Bayesian"			
Amplitude (A)	0.547	0.009	0.009
t_0 (ns)	449.76	0.059	0.060
T_{ion} (keV)	4.636	0.183	0.174
Scatter coef.	0.649	0.313	0.309
χ^2/ndof	0.335		

The values for the parameters obtained by the two methods shown in Table I are in agreement within the parameter uncertainties. The minimum χ^2 values per degree-of-freedom are similar, however the interpretation of this quantity for the "Bayesian" fit is difficult due to the very non-linear nature of the fits. The residuals, **s-Mh**, for each method are in agreement and are of order 1% of the maximum signal value, as shown in Fig. 1.

The uncertainty estimate for using the "Bayesian" analysis is roughly 3 times larger than for the "Exact" analysis. This is due to the inclusion of the IRF uncertainties and a rigorous method for combining uncertainties of many "bins" of signal and IRF as dictated by the model parameters. In particular, the parameters T_{ion} and scattering coefficient are significantly different, reflecting the sensitivity of these parameters to the IRF. The very large uncertainty of the scattering coefficient is likely due to the over estimate of the IRF long-time tail uncertainties, a result of this simple model of covariance.

The residual also indicates the possibility that the IRF used has systematic departures from the underlying "exact" IRF in the signal peak region (indicated by large, non-statistical departures of the signal from the fit). There is also short-time coherent "noise" that could be due to the detailed behavior of the digitizers.

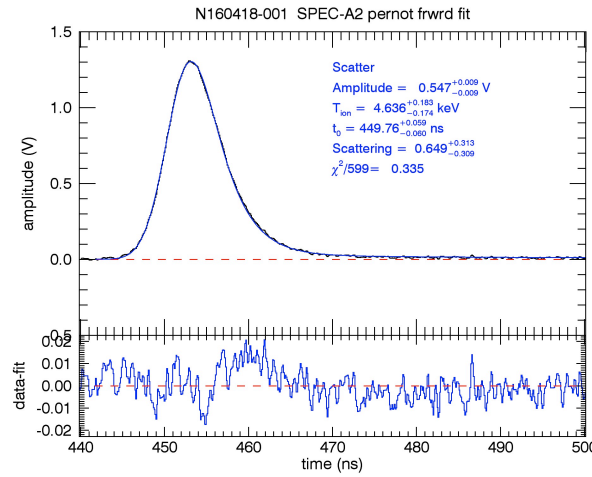

Figure 1 Result of "Bayesian" method for the Alcove nTOF on shot N160418-001, in the top panel the black histogram shows the data recorded on the shot, the blue function is the fit result. The lower panel shows the residual of the data-fit.

VI. CONCLUSION

The Bayesian analysis of Pernot has been implemented and tested using NIF nTOF spectrometer data in the full analysis structure. The results agree with the previous "forward fit" analysis that assumes perfect knowledge of the IRF. The uncertainty estimates using the Bayesian analysis are a factor of 3 larger than those of the "exact" analysis, a result that was anticipated from numerical studies of the "exact" analysis performance.

This method will provide a framework with which to investigate the elements of IRF construction leading to large uncertainties in model parameters, and provide insight in nTOF detector design and operations.

For more elaborate models extracting neutron spectrum cumulants identifiable with aspects of capsule performance, the methodology provided by the Bayesian analysis will help estimate the expected uncertainties of these cumulants and further guide the design and operations of neutron spectrometers capable of detecting these subtle effects.

[1]J. D. Lindl, *et al.*, Nucl. Fusion **51**, 094024 (2011).
[2]M. J. Edwards, *et al.*, Phys. Plasmas **20**, 070501 (2013).
[3]R. A. Lerche, *et al.*, Appl. Phys. Lett. **31**, 645 (1977).
[4]B. A. Remington, *et al.*, Rev. Sci. Instrum. **61**, 3128 (1990).
[5]T. J. Murphy, *et al.*, Rev. Sci. Instrum. **66**, 930 (1994).
[6]David H. Munro, Nucl. Fusion **56.3**, 036001 (2016).
[7]R. Hatarik, *et al.*, J. Appl. Phys. **118**, 184502 (2015).
[8]T. J. Clancy, *et al.*, Proc. of SPIE **9211**, 92110A (2014).
[9]R. Hatarik, *et al.*, Plasma and Fusion Research **9**, 4404104 (2014).
[10]V. Y. Glebov, *et al.*, Rev. Sci. Instrum. **83**, 10D309 (2012).
[11]G. P. Grim, *et al.*, Proc. of SPIE **8854**, 88540G (2013).